Progress in Additive Manufacturing
https://doi.org/10.1007/s40964-024-00614-z

FULL RESEARCH ARTICLE

High-performance thermoplastics obtained by fused filament fabrication: effects of harsh environmental conditions of power transformers

Catarina Costa[1] · Pedro Lopes[1,2] · João Castro[1] · João R. Matos[1] · Helena Lopes[3] · Joana R. Gouveia[1] · Sara M. Pinto[1] · Inês Ribeiro[1] · Luís Oliveira[1] · Thiago Assis Dutra[4]

Received: 11 December 2023 / Accepted: 19 March 2024

Abstract

In the evolving landscape of power transformers, the integration of advanced technologies, such as high-performance polymers obtained by Fused Filament Fabrication (FFF), is crucial. This study investigates the compatibility and performance of various 3D-printed polymer materials—Biofila, polyvinylidene fluoride (PVDF), polyphenylene Sulfone (PPSU), polyetheretherketone (PEEK), polyetherimide (ULTEM 1010), and polyetheretherketone reinforced with 20% glass fiber (PEEK-GF20) for use in power transformer components. Through oil compatibility, dielectric strength, and kerosene compatibility evaluations, the study gauges their suitability for this application. The results reveal that PPSU, PEEK, and ULTEM 1010 exhibit promising characteristics, specifically in regard to dielectric breakdown voltage and kerosene and insulating oil compatibility. In contrast, Biofila presented severe cracking when exposed to the mineral oil and PVDF and PEEK-GF20 fall short in terms of dielectric strength, rendering them unsuitable. Kerosene compatibility assessments show minimal material changes, confirming that all studied materials have good resistance to this drying agent, commonly used on power transformers. This research aims to provides essential insights into material selection for a new generation of power transformer parts.

Keywords Additive manufacturing · Fused filament fabrication · Mineral oil compatibility · Dielectric breakdown · Kerosene compatibility · Power transformers

C. Costa, P. Lopes, J. Castro, J. R. Matos, H. Lopes, T. A. Dutra, contributed equally to this work.

✉ Pedro Lopes
pmlopes@inegi.up.pt

Catarina Costa
clcosta@inegi.up.pt

João Castro
jcastro@inegi.up.pt

João R. Matos
jrmatos@inegi.up.pt

Helena Lopes
helena.lopes@efacec.com

Joana R. Gouveia
jrgouveia@inegi.up.pt

Sara M. Pinto
smpinto@inegi.up.pt

Inês Ribeiro
iribeiro@inegi.up.pt

Luís Oliveira
loliveira@inegi.up.pt

Thiago Assis Dutra
thiagoassis.dutra@gmail.com

[1] INEGI- Instituto de Ciência e Inovação em Engenharia Mecânica e Engenharia Industrial, FEUP Campus, Rua Dr. Roberto Frias, 400, Porto 4200-465, Portugal

[2] University of Porto, Praça de Gomes Teixeira, Porto 4099-002, Portugal

[3] EFACEC, Parque Empresarial Arroteia Rua Poente, São Mamede Infesta, 4465-591 Porto, Portugal

[4] C-MAST - Centre for Mechanical and Aerospace Science and Technologies, Universidade da Beira Interior, Rua Marquês d'Avila e Bolama, 6201-001 Covilhã, Castelo Branco, Portugal

Published online: 17 April 2024

1 Introduction

In recent years, there has been a remarkable evolution in products, machines, and manufacturing processes, driven by the advancement of digital technologies and the emergence of Industry 4.0. In this new era, the integration of advanced technologies has led to the concept of Transformer 4.0, a new generation of power transformers with superior performance characteristics. The improvement of reliability and the increase in efficiency are crucial objectives in the development of these systems [1, 2].

Power transformers are one of the most important equipment on the electricity grid, enabling the transmission and distribution of electrical energy. The main function of these machines is to allow the transfer of electrical energy between circuits with different voltages. Over the years, new materials and construction solutions have been developed, focusing mainly on the active part of the power transformer as opposed to its insulation system composed of cellulosic materials. Nowadays, as a large part of power transformers are reaching their expected life [3], and new manufacturing technologies are available, a research opportunity emerges for the application of new materials in these pieces of equipment.

Additive manufacturing (AM) technologies showed their potential to produce new parts for power transformers by leveraging the increased complexity, functionality, and operational performance of components that new designs can provide [4, 5]. Not specifically related to the technological process, but to the technology, AM can create opportunities for power transformers such as decentralized production, on-demand, low lead time and geographically close to customer replacement parts production, digital stock, and further digitalization of the manufacturing process [6]. The digital process aims to achieve a zero defect-based approach [7].

High-performance polymers have gained some attention as potential insulation materials due to their desirable electrical, mechanical and thermal properties [8, 9]. Their lightweight nature and chemical resistance make them attractive candidates for the development of high performance transformer components [10, 11].

There is an established knowledge on the literature, related to the ageing of mineral oil in transformers and the associated physical and dielectric effects on the traditionally manufactured insulating components, made mainly of cellulose paper or wood, and on the actual power transformer performance [12–15]. However, for polymeric materials, even-tough some work has been carried out such as in Ref. [16] it appears to be mainly early and exploratory work. For instance, in Ref. [17], the dielectrical and thermal properties of FFF produced Polycarbonate (PC), polyethylene terephthalate glycol (PETG) and acrylonitrile butadiene styrene (ABS-T) are evaluated. In Ref. [18], the same assessment is conducted for polylactic acid (PLA).

On the other hand, there are several investigations on high performance polymers. In Ref. [19] and [20], the authors investigated the effect of printing parameters on the geometrical and mechanical properties of polyetheretherketone (PEEK) and polyetherimide (PEI) 3D printed parts. Their work provided contributions to both the academy and industry, given the difficulties related to the 3D printing of materials that possess high melting temperatures. Although there have been studies to evaluate the dielectric behavior of printed polymers, there is not much work related to the compatibility with the transformer's products or the dielectric strength of different high performance polymers. The characterization and compatibility assessment of these polymers are essential to ensure their suitability for demanding power applications.

Thus, the present work focuses on investigating the effects of critical environmental conditions on high-performance 3D printed polymers for transformer applications. The study encompasses a comprehensive evaluation of various thermoplastic polymers, including Biofila, polyvinylidene fluoride (PVDF), polysulfone (PSU), polyphenylsulfone (PPSU), PEEK, PEI-ULTEM 1010, and glass fiber reinforced PEEK (PEEK-GF20). To assess the performance and suitability of these materials, a series of tests was conducted. The tests included oil compatibility, dielectric tests, and kerosene compatibility evaluations.

Understanding the behavior and performance of these 3D printed polymers under critical environmental conditions is crucial to their successful application in power systems. The results obtained from the conducted tests provide valuable insight into the compatibility, electrical insulation properties, and response to environmental stressors, enabling informed material selection and design considerations for high performance transformer components.

2 Materials and methods

2.1 Materials

The performance and longevity of power transformers is highly dependent on the materials used in their construction. High-performance polymers or polymer-based composites, which have the potential to be used as advanced Fused Filament Fabrication (FFF) materials [21–37], are excellent options to satisfy the demanding requirements of power transformer applications since they exhibit unique traits such as high chemical and electrical resistance, mechanical strength, thermal stability, and reduced weight. The materials investigated in this study are as follows:

- Biofila;
- polyvinylidene fluoride (PVDF);
- polyphenylsulfone (PPSU);
- polyetheretherketone (PEEK);
- polyetherimide (PEI)-ULTEM 1010;
- PEEK-GF20 (PEEK reinforced with 20% glass fiber).

These materials were selected because they represent a diverse set of polymers with unique properties. In conformity with the power transformer's components requirements, it is essential that the considered materials have high dielectric strength, good chemical resistance and strong mechanical properties.

Biofila is a biopolymer produced out of renewable material (lignin, wood, stark) that are not included on the food chain. These type of filaments do not depend on raw oil prices and speculation, therefore can be seen as a safer option that has less impact on the environment as well. Nevertheless, the work developed within 3D printed Biofila is limited. PVDF is an organic polymer known to be resistant to alcohols, oils, strong acids, halogen and basic solutions [38]. PPSU is a heat-resistant polymer with good mechanical and dielectric properties, as well as chemical resistance, usually used to produce membranes for filtration, pervaporation and gas separation [39–41]. PEEK is extremely resistant to chemical and thermal degradation. It resists to several solvents except to sulphuric acid [42]. The PEEK-GF20 presents higher tensile and flexural modulus when compared to PEEK [43]. ULTEM 1010 is a thermoplastic with high mechanical strength and chemically resistant to hydrocarbons, automotive fluids, alcohols and aqueous solutions. It shows stable dielectric breakdown [44].

Table 1 compares the chosen materials to the filaments used for general purpose commonly known PLA, ABS and PET-G. The mechanical properties were collected from technical sheets from the supplier 3DxTech^{TM}. The dielectric strength and chemical resistance is not provided. Several researches were studied [38, 45, 46], yet there is not much information available about the dielectric strength, neither about the chemical compatibility of these thermoplastics, specially when subjected to insulation oil and kerosene.

The work described in this article intends to characterise the chemical resistance of high performance 3D printed materials when exposed to power transformer insulating oil and to kerosene (the drying agent used on power transformer components). Besides, the dielectric strength after oil exposure is assessed. The results expect to contribute for further developments on the deployment of the use of new materials and technologies on the power transformers industry.

2.2 Methods

To assess the suitability of the studied materials for their application in power transformer insulation systems, it is necessary to consider two specific characteristics to allow correct operation of the transformer: (i) electrical insulation capacity, measured through the dielectric strength, and (ii) compatibility with oil and other agents such as kerosene.

Any material that integrates the insulating system in a power transformer must ensure insulation between turns, and between the windings and the magnetic circuit, avoiding direct contact between conductive components.

In the case of oil-immersed distribution transformers, it is necessary to ensure that the insulating material is compatible

Table 1 Mechanical properties, dielectric strength and chemical resistance of the selected materials compared to PLA, ABS and PET-G. (NT—not tested. No information provided on the supplier's technical sheet)

Material	Flexural strength [MPa]	Flexural modulus [MPa]	Tensile strength [MPa]	Tensile modulus [MPa]	Dielectric strength [kV/mm]	Chemical resistance
PLA	115 [47]	115 [47]	56 [47]	2865 [47]	25–34 [46]	Not resistant to: mineral oil, ethanol, gasoline [45, 48]
ABS	76 [49]	1985 [49]	42 [49]	1950 [49]	38–41 [46]	Not resistant to: mineral oil, acetone, gasoline[45, 48]
PET-G	72 [50]	1600 [50]	45 [50]	1650 [50]	21–40 [46]	Limited resistance to: mineral oil, acetone, gasoline[45, 48]
Biofila	NT	NT	51 [51]	2700 [51]	NT	NT
PVDF	50 [52]	1800 [52]	51 [52]	2450 [52]	10–27 [38]	Resistant to: benzene, glycerol, ethanol, methanol, propanol, mineral oil, paraffin oil [38, 53]
PPSU	110 [54]	2215 [54]	55 [54]	2310 [54]	14–20 [55]	Resistant to: gasoline, motor oil, transmission fluid [56]
PEEK	130 [57]	2700 [57]	100 [57]	3720 [57]	20 [58]	Resistant to: benzene, glycerol, methanol, diesel, mineral oil, parafin oil [59]
ULTEM 1010	110 [60]	2510 [60]	56 [60]	2500 [60]	16-33 [61]	Resistant to: benzene, engine coolant, motor oil, transmission oil [62]
PEEK-GF20	130 [63]	7625 [63]	105 [63]	7250 [63]	20 [58]	NT

with the oil contained in the tank, keeping the contamination level as low as possible to preserve the fluid quality.

Kerosene is used during the drying process of the cellulosic materials inside the power transformer. Therefore, compatibility of the samples with kerosene was also assessed.

2.2.1 Printing parameters

The samples were printed using FFF technology [21–37], which increasingly plays an important role in this power industry components, while at the same time research has increased in recent years. Given the characteristics of the materials adopted in the present work, to produce all the specimens the AON M2 3D printer was used, which has the following characteristics:

- Maximum bed temperature: 220 °C;
- Maximum extrusion temperature: 450 °C;
- Maximum chamber temperature: 135 °C;
- Build volume: 450 mm x 450 mm x 565 mm (length x width x height).

For each polymer examined, a set of printing tests was performed to identify a suitable combination of printing parameters. The considered printing parameters were:

- Bed temperature;
- extrusion Temperature;
- chamber temperature;
- speed;
- extrusion multiplier;
- layer height;
- layer width.

According to [64], the most influential printing parameters are layer height, extrusion temperature, speed, and bed temperature. Therefore, these parameters were tested starting from the supplier's recommendation and selected according to the best overall success of the printing process.

Ref. [65] highlights the importance of a heated chamber when printing high-performance polymers, allowing a higher control of the parts shrinkage, the interlayer stresses and the warpage and delamination-associated defects. The chamber temperature should be kept as close to the glass transition temperature (Tg) as possible taking into consideration the printer's limitations. In this study, the maximum chamber temperature allowed by the equipment was 135 °C , while the PPSU's Tg is 220 °C [54], PEEK's Tg is 143 °C [57], ULTEM 1010s Tg is 217 °C [60] and PEEK-GF20's Tg is 143 °C [63]. The suppliers do not recommend heated chamber to print Biofila and PVDF.

The extrusion multiplier influences the amount of material extruded while the nozzle travels at a given speed. Using a too high extrusion multiplier implies material overflow and lowering dimensional accuracy. In the opposite case, a very low extrusion multiplier results in worse stress–strain characteristics and voids [66]. The layer width defines the distance between consecutive lines of deposition. For the herein mentioned application and specially for the dielectric strength test, the samples must have as less voids and porosities as possible to assess the actual polymer dielectric behavior. Thus, these two printing parameters were selected based on the visual layer integrity and cohesion.

Table 2 summarizes the parameters adopted to produce the testing specimens for this work.

2.2.2 Geometry and printing strategies

Since the standards for oil compatibility and dielectric tests do not require a specific geometry, the samples were defined as rectangular shapes with dimensions of 100 mm x 50 mm x 1 mm, 100 mm x 50 mm x 2 mm, and 100 mm x 50 mm x 6 mm, as displayed in Fig. 1. The surface area of each specimen is 10,300 mm^2, 10,600 mm^2 and 11800 mm^2, respectively.

The printing strategy for the samples involved varying the infill orientations based on their thickness. For samples with a thickness of 1 mm, an infill orientation of 0° was adopted. For those with a thickness of 2 mm, infill orientations of 0°, 90°/0°, and 0°/90° were used. For samples with a thickness of 6 mm, an infill orientation of 45°/-45° including one perimeter was adopted. Figure 2 summarizes the adopted printing strategies.

Table 2 Parameters employed for each polymer printed (RT = Room temperature)

Material	Biofila	PVDF	PPSU	PEEK	ULTEM 1010	PEEK-GF20
Bed temperature [°C]	60	90	160	220	160	155
Extrusion temperature [°C]	210	265	400	420	370	375
Chamber temperature [°C]	RT	RT	135	135	135	135
Speed [mm/s]	45	5	16	5	20	10
Extrusion multiplier	1.0	0.87	0.90	0.87	0.94	0.80
Layer height [mm]	0.3	1.0	1.0	1.0	1.0	1.0
Layer width [mm]	Automatic	1.6	1.6	1.6	1.6	1.6

Fig. 1 Sample PVDF-4

Table 3 details the samples that were subjected through oil compatibility and/or dielectric strength tests and to the kerosene compatibility assessment.

The kerosene compatibility test standard, similarly to the oil compatibility test, does not require a specific geometry. Therefore, the adopted geometry was similar to a dog bone shape, as displayed in Fig. 3, considering the future intention of performing mechanical assessments on these samples. Each sample had a thickness of 7 mm and a theoretical surface area, in contact with kerosene, of 8246 mm^2.

2.3 Oil compatibility test

Insulating mineral oils are commonly used in electrical equipment employed in the generation, transmission, distribution, and general utilities of electrical energy. Maintaining oil quality is fundamental to ensure reliability throughout electrical equipment operation.

The oil compatibility test was designed to evaluate the compatibility between the material and the insulating mineral oil (Nytro Taurus). For each assessment, two beakers were prepared: one with 800 ml of insulating oil as the control and another beaker with the same amount of oil and two samples. The strategy of including two samples in a beaker, one with 1 mm and the other with 2 mms, was used to better utilize the available space inside the oven. The beakers were placed in a ventilated oven at 100 °C for 164 h, to simulate ageing. The time and temperature defined for the ageing procedure was defined internally by EFACEC, the power

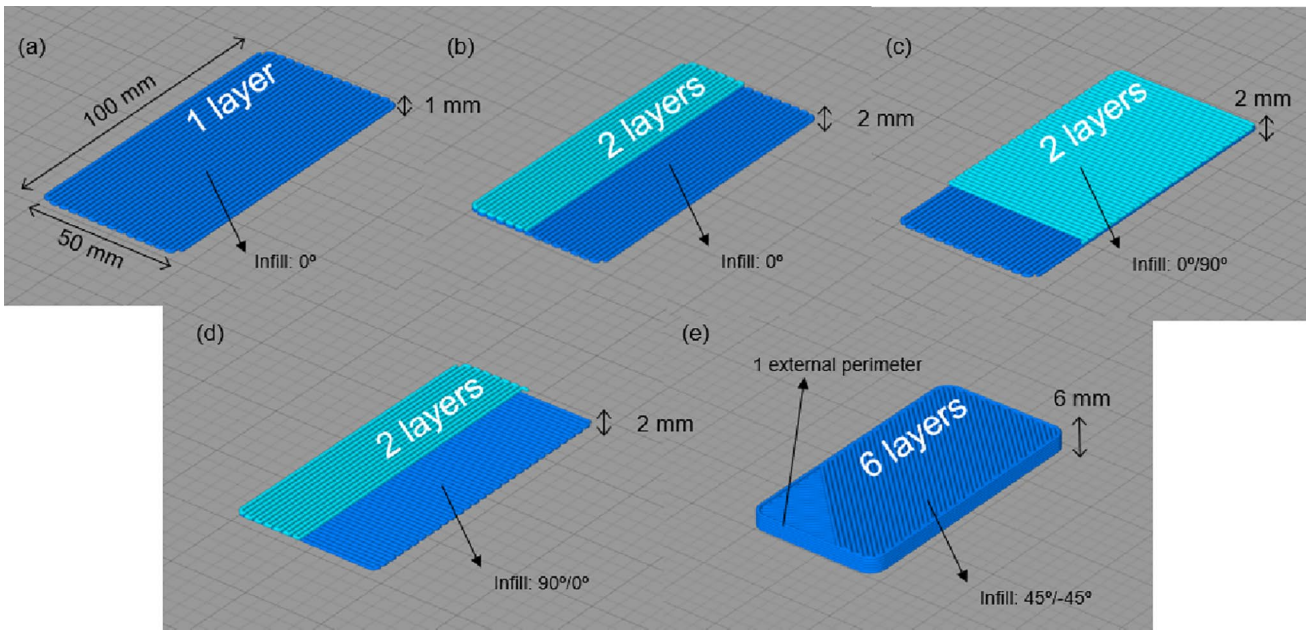

Fig. 2 Printing strategies for: (a) Specimen 100 mm x 50 mm x 1 mm; (b) Sample 100 mm x 50 mm x 2 mm with 0° infill; (c) Sample 100 mm x 50 mm x 2 mm with 0°/90° infill; (d) Sample 100 mm x 50 mm x 2 mm with 90°/0° infill and (e) Sample 100 mm x 50 mm x 6 mm

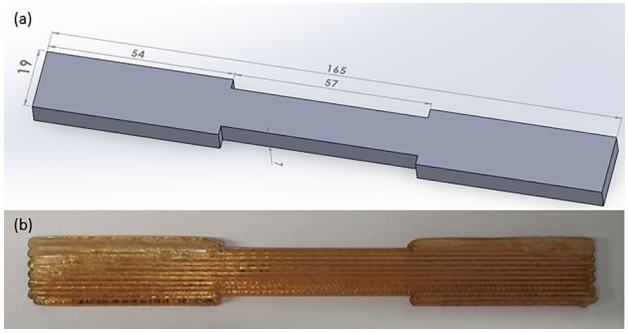

Fig. 3 (a) Dog bone samples' dimensions; (b) Sample ULTEM 1010-8

Table 3 Characterization of the tested samples

Material	Sample	Geometry	Thickness [mm]	Infill Orientation
Biofila	1 and 2	Rectangular	6	+45°/-45°
PVDF	1, 2 and 3	Rectangular	1	0°
	4		2	90°/0°
	5			0°
	6			0°/90°
PPSU	1,2 and 3	Rectangular	1	0°
	4		2	0°
	5			90°/0°
	6			0°/90°
	7,8 and 9	Dogbone	7	0°
PEEK	1,2 and 3	Rectangular	1	0°
	4		2	0°/90°
	5			0°
	6			90°/0°
	7,8 and 9	Dogbone	7	0°
ULTEM 1010	1, 2 and 3	Rectangular	1	0°
	4		2	0°/90°
	5 and 6			0°
	7, 8 and 9	Dogbone	7	0°
PEEK-GF20	1,2 and 3	Rectangular	1	0°
	4		2	90°/0°
	5 and 6			0°

transformers producer, which were developed considering several energy sector applicable standards.

After the ageing period, the oil from each container was analyzed to assess each polymer degradation. The following tests were conducted:

- Color and appearance assessment;
- Water content analysis;
- Acidity level determination;
- Interfacial tension measurement;
- Dissipation factor (tgδ) measurement;
- Disruptive tension measurement (in accordance with IEC 60422 [67]);
- Dissolved gas analysis (DGA) of gases dissolved in oil (in accordance with IEEE C57.104 [68]).

The test results provide insight into any changes in the properties of the insulating oil as a result of the interaction with the polymer.

2.3.1 Requirements

The geometry of the samples was determined by the container used for the tests. The samples had dimensions of 100 mm x 50 mm x 1 mm, 100 mm x 50 mm x 2 mm, or 100 mm x 50 mm x 6 mm (length x width x thickness), as previously shown in Fig. 1. The test plan involved the testing of six samples for each material.

2.4 Dielectric test

The dielectric test aimed to characterize the dielectric strength of the studied materials as a solid insulating material, using the relevant power frequencies in accordance with the standard ASTM D149-09 [69] Method A—Short-Time Test.

According to the standard, the dielectric test should mimic the application conditions as much as possible. The work carried out in [70] concluded that the sample density affects the dielectric strength of the material. Hence, the samples exposed to dielectric experiments were aged and tested in terms of oil compatibility before. Consequently, the dielectric behavior of the samples might be influenced by previous exposures, and therefore, the breakdown tension values might not be similar to the theoretical properties. The results should be compared between themselves for the sake of the power transformer application and not extrapolated to different dielectric assessments using different surrounding medium, electrodes, or methods.

An alternating voltage at a commercial power frequency of 60 Hz was applied to a test specimen submerged in insulating oil using two Type 3 electrodes from a DTA equipment with a voltage rating of 80 kV.

The voltage was gradually increased from zero until dielectric failure occurred. The dielectric failure is evidenced by a rapid increase in the conductance of the dielectric under test, which limits the electric field that can be sustained.

The measured value obtained from the test was the dielectric breakdown voltage through the thickness of the test sample, which characterizes the dielectric strength of the polymer that is usually expressed in kV/mm. This voltage represents the maximum voltage that the material can

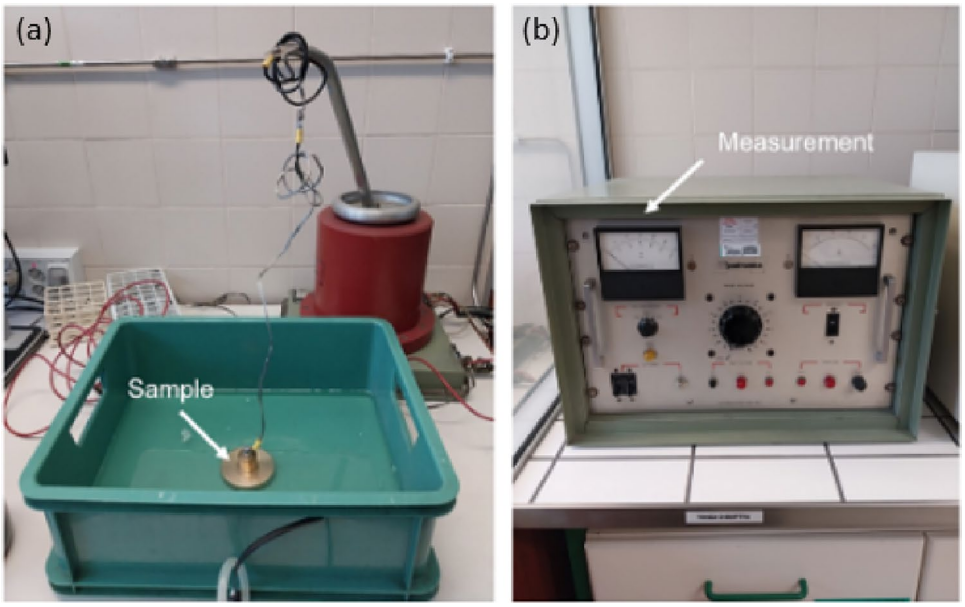

Fig. 4 Dielectric strength test setup: **a** sample and **b** measurement equipment

withstand without experiencing electrical breakdown. The test setup is depicted in Fig. 4.

2.4.1 Requirements

The dielectric breakdown voltage can be influenced by the electrodes material and geometry, sample thickness, temperature, testing time, wave form, current frequency, and surrounding medium. All tests were done using the same electrodes, applied current, and submerging insulating oil. Temperature variations were not taken into account as no major changes were recorded during the test. In regard to thickness changes, more than one thickness was experimented for each material for a more comprehensive comparison.

The ASTM D149-09 standard [69] does not specify a particular geometry for the samples, but it requires the specimens to be larger than the electrodes to avoid measuring the dielectric strength of the insulating oil. After consulting the dielectric strength per thickness in the literature (Table 1), the maximum thickness to be tested was set to 2 mm for all materials except Biofila, due to a lack of information on its dielectric strength. Because of the maximum voltage rating of the equipment used, higher thicknesses could compromise the results.

2.5 Kerosene compatibility test

The drying process in power transformers aims to remove water from the interior of the insulating system, which is typically composed of cellulosic materials, such as cardboard or wood laminates. The presence of water significantly reduces the dielectric strength and accelerates the aging of the insulating structure, compromising the lifespan of the transformer. According to [71], the moisture content present in a new transformer unit should typically not exceed 0.5%. To achieve this, it is necessary to submit the transformer to an efficient drying process.

One of the more effective drying processes applied in power transformer components is the Vapor Phase. It involves injecting a heated solvent at low pressures into a sealed autoclave, which promotes the removal of water molecules from the insulating components. Kerosene is used as solvent due to its significantly lower vapor pressure compared to water.

Generally, the drying cycle consists of at least five main steps:

- Evacuation: Pressure is reduced from atmospheric to around 10 mbar inside the autoclave.
- Heating: It consists of the evaporation of kerosene and its injection into the autoclave. Kerosene steam condenses upon contact with surfaces at lower temperatures, releasing a high amount of energy that, when transmitted to the insulating masses, vaporizes the water inside, forcing it to leave. At this stage, the average temperature of the insulating materials should not exceed 120 °C.
- Removal: Pressure in the autoclave is reduced, promoting the removal of water, kerosene and other residues from the insulation system components.
- Distillation: Separates kerosene from other impurities mixed with it during the removal stage, such as water, oil, and solid particles. This process cleans the kerosene, restoring its properties as a heat transfer agent. It is recommended that distillation occurs at the end of the initial heat-removal cycles.

- Vacuum: Autoclave pressure drops to the lowest value allowed by the vacuum system to ensure the greatest pressure differential between the interior of the insulation components and the surrounding environment, facilitating the removal of remaining water.

Figure 5 illustrates the steps of the drying process. The distillation step is not illustrated in the figure. The number of consecutive heating and removal cycles applied is selected according to the mass of the insulating materials to be dried.

2.5.1 Requirements

For the test herein studied, three Heating-Removal-Distillation (Fig. 5) stages were adopted. The drying cycle is detailed in Table 4. The duration of each stage was defined internally by EFACEC based on previous experience. Three samples of each material should be considered for significant results.

The total drying process time was 41 h. The kerosene compatibility result was based on the comparison of the sample weight and dimensions before and after the drying process, implying contamination or deterioration of the material.

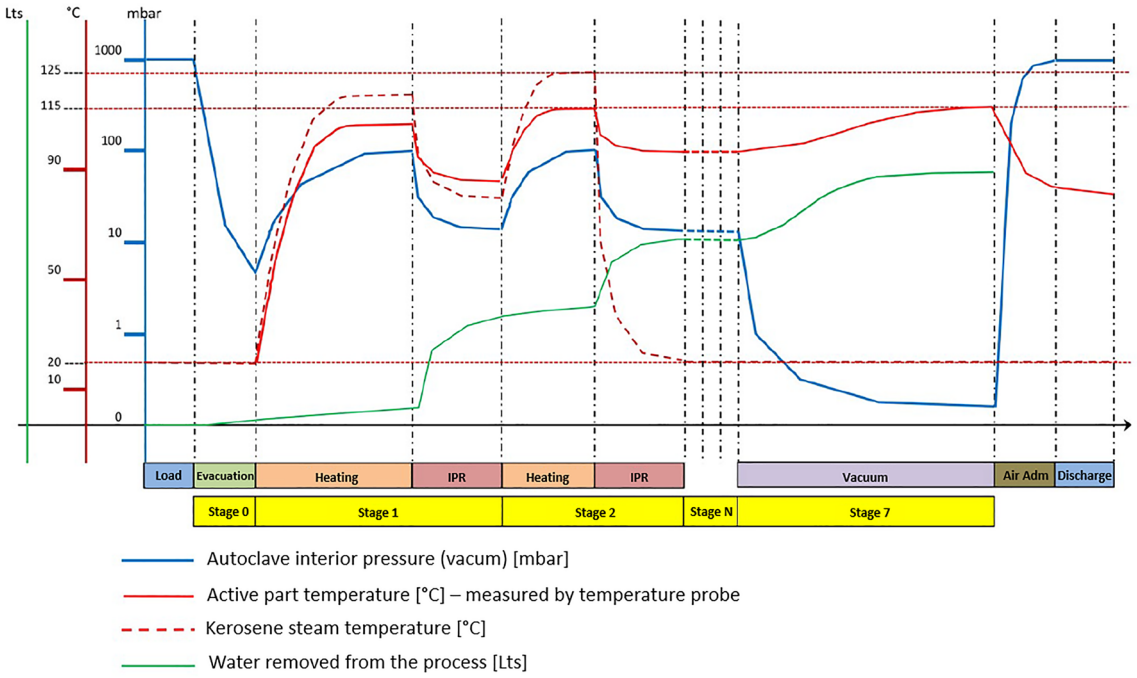

Fig. 5 Example of Vapor Phase drying cycle

Table 4 Vapor Phase drying process applied to the specimens

Stage		0	1	2	3	4
Evacuation	Duration [h]	2				
	Criterion - Pressure [mbar]	7				
Heating	Duration [h]		9	3	2	
	Criterion - Probe temperature [°C]		100	115	115	
Removal	Duration [h]		2	1	1	
	Criterion - Pressure [mbar]		20	20	20	
Distillation	Duration [h]		4	2		
Vacuum	Walls heating duration [h]					9
	Duration without walls heating [h]					6
	Criterion - Pressure [mbar]					0.5
	Criterion - Extracted water rate [g/ton h]					20

3 Results and discussion

3.1 Oil compatibility test

The results from the physical and chemical tests on the materials after oil exposure are stated in Table 5, while Table 6 detail the results of the dissolved gases assessment on the oil.

According to IEC 60422 [67], no significant changes were observed on the insulation oil after exposure to the proposed polymers.

Biofila has shown a slight increase in CO_2 and CO content, as can be seen in Table 6. PVDF presented an increase in the content of H_2 and CO. PPSU, PEEK and ULTEM 1010 did not present any significant alteration on the dissolved gases on the insulation oil. There was also an increase in the content of H_2, C_2H_6, CH_4 and CO in the PEEK-GF20 specimens.

However, all these gains are below the typical values for gases produced in in-service transformers (aged oil) mentioned in the standard IEEEC 57.104 [68]. PPSU, PEEK, and ULTEM 1010 did not show significant influences on the physical properties of the oil and the dissolved gases. Even though all polymers have shown compliant parameters, Biofila samples were severely deformed and presented significant cracks (see Fig. 6). Therefore, this material was disregarded and no more samples were tested.

Table 5 Physical and chemical tests for evaluation of oil compatibility

Material	Sample	Color and appearance	Water content	Acidity level [mgKOH/kg]	Interfacial tension [mN/m]	tgδ	Disruptive tension [kV]
Biofila	Control	0.2	15.0	0.005	41.4	0.00053	69.7
	1 and 2	0.2	6.3	0.043	35.8	0.00104	64.1
PVDF	Control	0	26.4	0.005	37.4	0.00055	56.9
	1 and 4	0	22.0	0.006	39.2	0.00153	64.5
	Control	0	18.5	0.007	31.4	0.00302	65.4
	2 and 5	0.5	13.9	0.011	28.7	0.00406	72.1
	Control	0	12.1	0.005	41.6	0.00040	63.3
	3 and 6	0	10.2	0.005	41.5	0.000132	75.7
PPSU	Control	L0.5	15.3	0.007	36.1	0.00081	53.7
	1 and 4	0	19.3	0.005	36.5	0.00063	71.6
	Control	0	14.4	0.005	35.7	0.00131	67.4
	2 and 5	0	16.1	0.005	34.9	0.000166	61.1
	Control	L0.5	12.7	0.020	30.4	0.00201	45.1
	3 and 6	L0.5	13.2	0.018	30.3	0.00268	38.5
PEEK	Control	0	26.4	0.005	37.4	0.00055	56.9
	1 and 4	0	16.4	0.005	38.2	0.00170	53.4
	Control	0	18.5	0.007	31.4	0.00302	65.4
	2 and 5	0.5	13.3	0.010	29.3	0.00497	73.5
	Control	0	12.1	0.005	41.6	0.00040	63.3
	3 and 6	0	12.7	0.005	42.3	0.00151	65.6
ULTEM 1010	Control	L0.5	15.3	0.007	36.1	0.00081	53.7
	1 and 4	0	7.8	0.005	36.6	0.00062	54.5
	Control	5	14.4	0.005	35.7	0.00131	67.4
	2 and 5	0	26.1	0.005	36.2	0.000161	32.6
	Control	L0.5	12.7	0.020	30.4	0.00201	45.1
	3 and 6	L0.5	21.6	0.019	31.8	0.00181	49.5
PEEK-GF20	Control	0	26.4	0.005	37.4	0.00055	56.9
	1 and 4	0	34.9	0.005	39.3	0.00041	50.4
	Control	0	18.5	0.007	31.4	0.00302	65.4
	2 and 5	0	20.5	0.009	33.3	0.00110	71.1
	Control	0	12.1	0.005	41.6	0.00040	63.3
	3 and 6	0	11.3	0.005	38.4	0.00035	64.5

Table 6 Dissolved gases in the oil compatibility tests

Material	Sample	H_2 [ppm]	O_2 [ppm]	N_2 [ppm]	CO_2 [ppm]	C_2H_4 [ppm]	C_2H_6 [ppm]	C_2H_2 [ppm]	CH_4 [ppm]	CO [ppm]	Total [%]
Biofila	Control	< 3	26329.8	55261.9	305.6	< 0.2	< 0.2	< 0.2	< 0.3	9.3	8.2
	1 and 2	<3	27728.4	57851.3	967.8	0.3	< 0.2	< 0.2	< 0.3	14.5	8.7
PVDF	Control	<3	23292.6	49883.8	319.4	0.2	< 0.2	< 0.2	< 0.3	12.3	7.4
	1 and 4	<3	27528.1	60472.1	394.4	0.3	< 0.2	< 0.2	< 0.3	14.5	8.8
	Control	<3	28532.28	59746.0	379.5	0.4	3.0	< 0.2	< 0.3	19.9	8.9
	2 and 5	11.1	30096.8	74352.5	472.6	0.9	0.9	< 0.2	< 0.3	47.3	10.5
	Control	<3	24438.2	47127.4	449.6	<0.2	< 0.2	< 0.2	< 0.3	9.0	7.2
	3 and 6	<3	29225.3	58529.0	409.2	0.2	< 0.2	< 0.2	< 0.3	11.1	8.8
PPSU	Control	<3	22818.4	48091.8	543.5	0.3	< 0.2	< 0.2	< 0.3	15.0	7.1
	1 and 4	4.4	17697.4	52181.1	429.8	0.5	0.8	< 0.2	< 0.3	36.2	7.0
	Control	<3	19348.6	41633.6	332.7	<0.2	< 0.2	< 0.2	< 0.3	9.4	6.1
	2 and 5	<3	15689.6	35779.4	295.2	0.3	< 0.2	< 0.2	< 0.3	13.3	5.2
	Control	<3	29353.8	63326.0	340.0	0.4	< 0.2	< 0.2	< 0.3	15.3	9.3
	3 and 6	9.2	23096.9	60800.7	444.4	0.8	0.9	<0.2	< 0.3	51.3	8.4
PEEK	Control	<3	23292.6	49883.8	319.4	0.2	<0.2	<0.2	< 0.3	12.3	7.4
	1 and 4	<3	25916.6	54536.4	307.1	0.2	<0.2	<0.2	< 0.3	10.2	8.1
	Control	<3	28532.2	59746.0	379.5	0.4	3.0	<0.2	< 0.3	19.9	8.9
	2 and 5	4.9	30407.7	70136.9	441.9	0.7	2.3	<0.2	< 0.3	43.8	10.1
	Control	<3	24438.2	47127.4	449.6	<0.2	<0.2	<0.2	< 0.3	9.0	7.2
	3 and 6	<3	28967.0	53988.1	439.3	<0.2	<0.2	<0.2	< 0.3	8.3	8.3
ULTEM 1010	Control	<3	22818.4	48091.8	543.5	0.3	<0.2	<0.2	< 0.3	15.0	7.1
	1 and 4	<3	25000.2	57230.8	391.9	0.3	<0.2	<0.2	< 0.3	17.6	8.3
	Control	<3	19348.6	41633.6	332.7	<0.2	<0.2	<0.2	<0.3	9.4	6.1
	2 and 5	<3	17268.6	40725.4	305.5	0.4	0.8	<0.2	<0.3	17.7	5.8
	Control	<3	29353.8	63326.0	340.0	0.4	<0.2	<0.2	<0.3	15.3	9.3
	3 and 6	12.8	19648.8	58794.2	462.2	0.9	3.1	<0.2	<0.3	73.4	7.9
PEEK GF20	Control	<3	23292.6	49883.8	319.4	0.2	<0.2	<0.2	<0.3	12.3	7.4
	1 and 4	<3	19700.4	44311.1	285.0	0.3	<0.2	<0.2	<0.3	14.8	6.4
	Control	<3	28532.2	59746.0	379.5	0.4	3.0	<0.2	<0.3	19.9	8.9
	2 and 5	6.4	27164.5	72176.2	432.7	0.6	11.3	<0.2	3.5	58.2	10.0
	Control	<3	24438.2	47127.4	449.6	<0.2	<0.2	<0.2	<0.3	9.0	7.2
	3 and 6	<3	27479.9	54172.0	408.5	0.3	<0.2	<0.2	<0.3	10.8	8.2

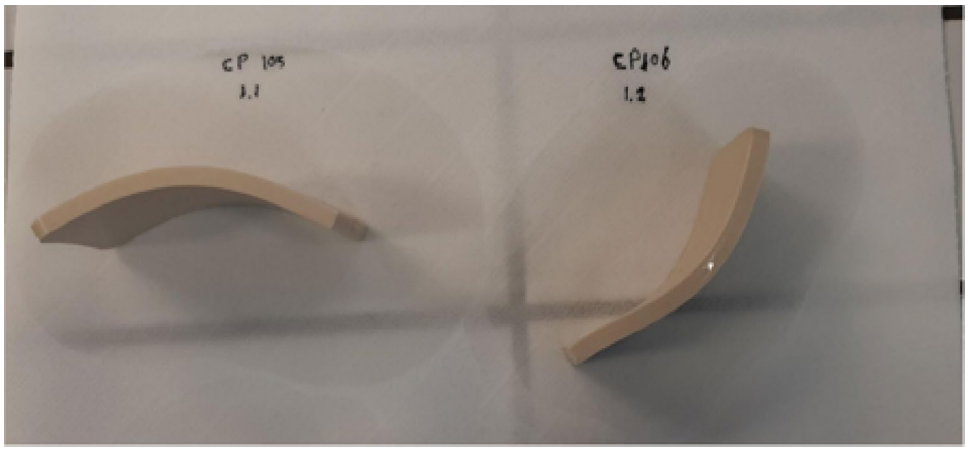

Fig. 6 Biofila specimens after aging

3.2 Dielectric test

Concerning the dielectric test, a container with only oil and no sample in between the electrodes was tested for distances of 1 and 2 mm. This distance corresponds to the thickness of the sample when it is placed between the electrodes. This measurement does not determine the oil dielectric strength since the standard is only applicable to solid materials. Nevertheless, this value sets a reference for each thickness, that gives further insight to the comparison of results obtained for the different polymers investigated herein. The tested specimens are those previously detailed in Table 3, from the materials PVDF, PPSU, PEEK, ULTEM1010, and PEEK-GF-20. Table 7 details the dielectric breakdown results for each sample.

The dielectric strength test ends when a perforation of the sample is achieved, as shown in Fig. 7, or a deviation of the electric arc around the sample occurs.

Table 8 condenses the average dielectric breakdown results and the percentage of variation. The "Variation from the oil dielectric breakdown" column characterizes the difference between the average measurement recorded for that material and thickness and the dielectric breakdown measured with only oil in between the electrodes at a distance equal to the sample's thickness. It is important to highlight that a negative variation in the respective oil breakdown means that the sample assessment withstood less voltage than the oil experiment itself.

For a distance of 1 mm between the electrodes, the dielectric breakdown for PPSU, PEEK, and ULTEM 1010 was very similar, reaching almost 30% above the comparison value of the mineral oil. Furthermore, the dielectric breakdown of specimens with a thickness of 2 mm was slightly lower for ULTEM 1010 (40 kV), while PEEK and PPSU reached 15% higher than the reference.

Figure 8 presents the results of the dielectric test for all the materials tested for the two thicknesses considered. The results from samples PEEK-GF20-1 and PEEK-GF20-4 were

Table 7 Dielectric breakdown results

Material	Sample	Dielectric Breakdown (kV)
PVDF	1	17.0
	2	15.5
	3	16.6
	4	28.7
	5	29.1
	6	29.5
PPSU	1	26.7
	2	28.8
	3	27.4
	4	39.8
	5	41.2
	6	40.9
PEEK	1	29.7
	2	27.5
	3	26.6
	4	41.9
	5	41.7
	6	39.8
ULTEM 1010	1	24.6
	2	25.5
	3	32.0
	4	41.2
	5	41.5
	6	37.3
PEEK-GF20	1	0.9
	2	15.6
	3	19.8
	4	1.8
	5	35.6
	6	37.5

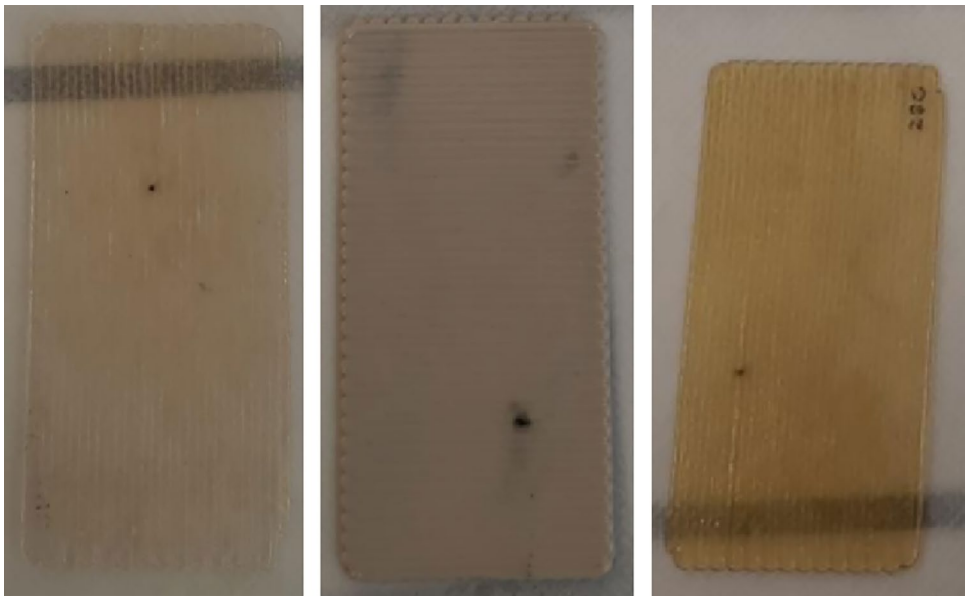

Fig. 7 Visible sample perforation due to dielectric test on specimen PPSU-6, PEEK-6, and ULTEM 1010-2 from left to right

Table 8 Average dielectric breakdown tension for specimens with thickness of 1 and 2 mm

Material	Thickness = 1 mm		Thickness = 2 mm	
	Average dielectric breakdown [kV]	Variation from the oil dielectric breakdown	Average dielectric breakdown [kV]	Variation from the oil dielectric breakdown
PVDF	16.37	–20 %	29.10	–19 %
PPSU	27.63	29 %	40.63	15 %
PEEK	27.93	30 %	41.13	16 %
ULTEM 1010	27.37	28 %	40.00	13 %
PEEK-GF20	17.70	–11 %	36.55	5 %

considered as outliers and therefore were not included in the average dielectric breakdown, as their values were much lower than those of the remaining measurements.

As mentioned above, the measurement performed using only the insulating oil does not refer to the actual dielectric strength of the fluid, since the applied standard is only valid for solid materials. However, it serves as a comparison of the remaining results.

As can be seen in Table 8, as well as in Fig. 8, the dielectric breakdowns of PVDF and PEEK-GF20 were, on average, lower than the measured breakdown voltage obtained for the insulating oil. Moreover, those two materials were verified as incompatible with the application and therefore were not considered for further testing. According to the dielectric results, for the samples with a thickness of 2 mm, no significant influence of the infill orientation was observed on the overall dielectric results.

3.3 Kerosene compatibility test

To evaluate the effect of kerosene, the samples were weighted and measured before and after exposure. Variations seem negligible. However, the samples were not sealed in vacuum between the kerosene exposure and the measurements. In an attempt to diminish the influence absorbed humidity has on the specimens weights they were dried, before the final weight measurement.

According to the drying specifications of the filament provider, the material should be exposed to 313.15 K cycle for 4 h. The heating and cooling rates were set to 3.5 K/min and − 2.3 K/min respectively, as can be seen in Fig. 9.

Table 9 reports the final results and comparisons of the mass. No dimensional changes were observed after exposure to kerosene. On average, PEEK had 0.04% of weight gain (9 mg), PPSU a 0.25% loss (58 mg), and ULTEM 1010 a 0.15% gain (34 mg). Since none of the results was significant enough to disregard any of the polymers, all tested materials were considered kerosene resistant.

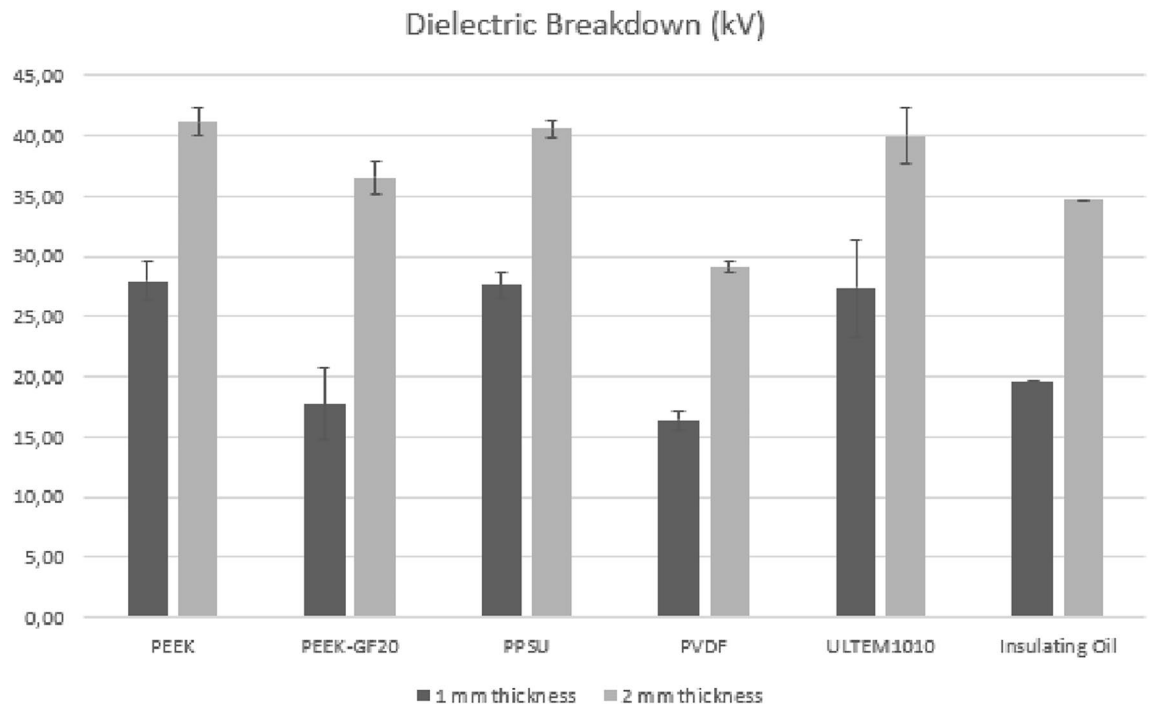

Fig. 8 Dielectric breakdown plot for PVDF, PPSU, PEEK, ULTEM 1010, PEEK-GF20 and oil for the samples with a thickness of 1 and 2 mm

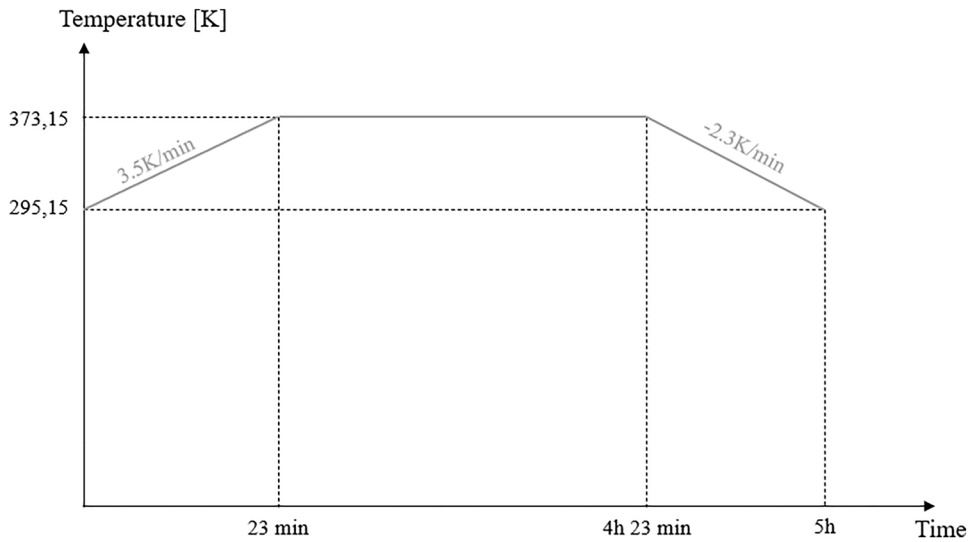

Fig. 9 Thermal cycle adopted to dry the specimens exposed to kerosene

4 Conclusions

In the present work, advanced polymers manufactured through 3D printing, including Biofila, PVDF, PPSU, PEEK, ULTEM 1010 and PEEK-GF20 were studied for their applicability in power transformers construction. To assess their suitability, oil compatibility, dielectric strength, and kerosene compatibility tests were performed.

Regarding oil compatibility, some properties such as appearance, water content, dissipation factor, and dissolved gas in the oil were analyzed to investigate possible contamination according to IEC 60422 [67] and IEEE C57.104 [68]. Increases in CO_2 and CO contents were verified for Biofila, and an increase in H_2 and CO content was verified for PVDF. An increase in H_2, C_2H_6, CH_4, and CO content was also verified for PEEK-G20.

Table 9 Samples dimensions and mass results before/after exposure to kerosene and after drying

Material	Sample	Before kerosene exposure	After kerosene exposure	After drying	Weight change after exposure	Weight change after drying
		Mass [g]	Mass [g]	Mass [g]	[%]	[%]
PEEK	1	21.88	21.88	21.88	0.02	0.02
	2	21.65	21.66	21.66	0.04	0.07
	3	21.74	21.75	21.75	0.03	0.04
PPSU	1	23.40	23.25	23.23	−0.65	−0.73
	2	22.44	22.46	23.44	−4.17	0.00
	3	23.38	23.39	23.38	0.05	−0.01
ULTEM 1010	1	22.58	22.60	22.59	0.07	0.04
	2	22.54	22.56	22.56	0.09	0.03
	3	22.59	22.68	22.67	0.42	0.38

Nevertheless, the observed increments were not meaningful compared to normal contamination on an operational power transformer.

Although Biofila did not present a significant variation in oil chemical appearance or content, the samples used in the oil compatibility tests were strongly damaged throughout the assessment, exhibiting warping and visible cracks. Hence, the material was not considered for the remaining tests. In total, six samples of each material were exposed to mineral insulating oil, except Biofila, which was tested with only two parts.

The dielectric strength was also explored. The same six samples of PVDF, PPSU, PEEK, ULTEM 1010, and PEEF-GF20 (three with a thickness of 1 mm and three with a thickness of 2 mm) previously exposed to mineral oil were evaluated. For comparison, dielectric breakdown measurements were performed with electrodes at the same distance as the thickness of the samples and without any material in between besides the insulating oil. Both PVDF and PEEK-GF20 exhibited lower average dielectric breakdown values than the reference measurement, thus these materials were discarded from further testing. No clear relation was observed between the infill orientation and the dielectric breakdown. The best dielectric breakdown results were achieved by PEEK with 27.93 kV for samples with 1 mm thickness and 41.13 kV for those with 2 mm.

The remaining materials were tested for kerosene compatibility, in which the dimensions and weight of the samples were measured before and after a drying process with kerosene injection. An additional thermal cycle recommended by the filament supplier was performed to dry the samples before the final weight measurement. For this test, three samples were used for each polymer. The weight changes were revealed to be marginal, as the maximum mass variation detected was 0.25% (58 mg) for PPSU. Based on these results, PEEK, ULTEM 1010, and PPSU were considered resistant to kerosene.

From the results presented here, at least three advanced polymer materials (PEEK, ULTEM 1010, and PPSU) have the basic requirements for application in power transformer insulation systems. Although a complete substitution of cellulosic materials for these materials still remains a challenge, due to the excellent insulation properties, availability, and low cost of paper and cardboard, these polymers combined with 3D printing technology present the potential to be a flexible solution to the development of quickly customizable components embedded with sensorization systems for the next generation of power transformers.

Acknowledgements The project TRF4p0–Transformer 4.0 leading to this work was co-financed by the European Regional Development Fund—ERDF, through COMPETE—Operational Program Competitiveness and Internationalization (POCI) and by the Foundation for Science and Technology under the MIT Portugal Program under POCI-01-0247-FEDER-045926. The author Thiago Assis Dutra also acknowledges the *Fundação para a Ciência e Tecnologia* (FCT) and R &D Unit *Centre for Mechanical and Aerospace Science and Technologies* (C-MAST) under grant numbers UIDB/00151/2020 (https://doi.org/10.54499/UIDB/00151/2020) and UIDP/00151/2020 (https://doi.org/10.54499/UIDP/00151/2020). On behalf of all authors, the corresponding author states that there is no conflict of interest.

Funding Open access funding provided by FCT|FCCN (b-on).

Data availability The authors confirm that the data studied on this work are available within the article. Raw or additional information might be available from the corresponding author, upon reasonable request.

References

1. Baduge SK, Thilakarathna S, Perera JS, Arashpour M, Sharafi P, Teodosio B, Shringi A, Mendis P (2022) Artificial intelligence and smart vision for building and construction 4.0: Machine and deep learning methods and applications. Autom Constr 141:104440. https://doi.org/10.1016/j.autcon.2022.104440
2. Silva H, Moreno T, Almeida A, Soares AL, Azevedo A (2022) A digital twin platform-based approach to product lifecycle management: Towards a transformer 4.0. In: Machado, J. et Al. Innovations in Industrial Engineering II. Lectures Notes in Mechanical Engineering. https://doi.org/10.1007/978-3-031-09360-9_2
3. Ma H, Saha TK, Ekanayake C, Martin D (2015) Smart transformer for smart grid–intelligent framework and techniques for power transformer asset management. IEEE Transactions on Smart Grid 6(2):1026–1034. https://doi.org/10.1109/TSG.2014.2384501
4. Wong KV, Hernandez A (2012) A review of additive manufacturing. International scholarly research notices 2012. https://doi.org/10.5402/2012/208760
5. Attaran M (2017) The rise of 3-d printing: The advantages of additive manufacturing over traditional manufacturing. Bus Horiz 60(5):677–688. https://doi.org/10.1016/j.bushor.2017.05.011
6. Borgue O, Stavridis J, Vannucci T, Stavropoulos P, Bikas H, Di Falco R, Nyborg L (2021) Model-based Design of AM Components to Enable Decentralized Digital Manufacturing Systems. In: Proceedings of the Design Society, vol. 1. Gothenburg, Sweden, pp. 2127–2136. https://doi.org/10.1017/pds.2021.474 . International Conference on Engineering Design (ICED21)
7. Powell D, Magnanini MC, Colledani M, Myklebust O (2022) Advancing zero defect manufacturing: A state-of-the-art perspective and future research directions. Comput Ind 136:103596. https://doi.org/10.1016/j.compind.2021.103596
8. Fink JK (2014) High Performance Polymers, 2nd edn. PDL Handbook Series. https://doi.org/10.1016/B978-0-323-31222-6.00006-6
9. Liu Z, Wang L, Hou X, Wu J (2020) Investigation on dielectrical and space charge characteristics of peek insulation used in aerospace high-voltage system. IEEJ Transactions on Electrical and Electronic Engineering. https://doi.org/10.1002/tee.23042
10. Lyu M-Y, Choi TG (2015) Research trends in polymer materials for use in lightweight vehicles. Int J Precis Eng Manuf 16:213–220. https://doi.org/10.1007/s12541-015-0029-x
11. Wypych G (2022). Handbook of Polymers. https://doi.org/10.1016/C2011-0-04631-8
12. Diwyacitta K, Prasojo RA, Harjo S (2017) Effects of Loading Factor in Operating Time on Dielectric Characteristics of Transformer Oil, Denpasar, Indonesia. https://doi.org/10.1109/ICHVEPS.2017.8225968 . 2017 International Conference on High Voltage Engineering and Power Systems (ICHVEPS)
13. Azis N, Zhou D, Wang ZD (2012) Operational Condition Assessment of In-service Distribution Transformers, Bali, Indonesia, pp. 1156–1159. https://doi.org/10.1109/CMD.2012.6416364. . 2012 IEEE International Conference on Condition Monitoring and Diagnosis
14. Tee S, Liu Q, Wang Z, Wilson G, Jarman P, Hooton R, Dyer P, Walker D (2015) Practice of IEC 60422 in Ageing Assessment of In-service Transformers, Pilsen, Czech Republic. The 19th International Symposium on High Voltage Engineering
15. Xiao M, Du BX (2016) Review of high thermal conductivity polymer dielectrics for electrical insulation. High Voltage 1(1):34–42. https://doi.org/10.1049/hve.2016.0008
16. Sekula R, Immonen K, Matsa-Kortelainen S, Kuniewski M, Zydron P, Kalpio T (2023) Characteristics of 3d printed biopolymers for applications in high-voltage electrical insulation. Polymers. https://doi.org/10.3390/polym15112518
17. Kalas D, Sima K, Kadlec P, Plansky R, Soukup R, Reboun J, Hamacek A (2021) Fff 3d printing in electronic applications: Dielectric and thermal properties of selected polymers. Polymers. https://doi.org/10.3390/polym13213702
18. Dichtl C, Sipple P, Krohns S (2017) Dielectric properties of 3d printed polylactic acid. Advances in Materials Science and Engineering. https://doi.org/10.1155/2017/6913835
19. Dutra TA, Costa C, Matos JR, Oliveira BF, Oliveira LM, Coutinho CP (2022) Effects of Printing Parameters on Geometrical and Mechanical Properties of 3D-Printed High-Performance Thermoplastics. Toward the Digitalization of Power Transformers, Lisbon, Portugal. https://doi.org/10.1115/IAM2022-91989. 2022 International Additive Manufacturing Conference
20. Magri AE, Vanai S, Vaudreuil S (2021) An overview on the influence of process parameters through the characteristic of 3d-printed peek and pei parts. High Performance Polymers 33. https://doi.org/10.1177/0954008321100996
21. Kulkarni P, Dutta D (1999) Deposition strategies and resulting part stiffnesses in fused deposition modeling. J Manuf Sci Eng 121(1):93–103. https://doi.org/10.1115/1.2830582
22. Ahn S-H, Montero M, Odell D, Roundy S, Wright PK (2002) Anisotropic material properties of fused deposition modeling ABS. Rapid Prototyping Journal 8(4):248–257. https://doi.org/10.1108/13552540210441166
23. Bellini A, Güçeri S (2003) Mechanical characterization of parts fabricated using fused deposition modeling. Rapid Prototyping Journal 9(4):252–264. https://doi.org/10.1108/13552540310489631
24. Carneiro OS, Silva AF, Gomes R (2015) Fused deposition modeling with polypropylene. Materials & Design 83:768–776. https://doi.org/10.1016/j.matdes.2015.06.053
25. Casavola C, Cazzato A, Moramarco V, Pappalettere C (2016) Orthotropic mechanical properties of fused deposition modelling parts described by classical laminate theory. Materials & Design 90:453–458. https://doi.org/10.1016/j.matdes.2015.11.009
26. Panda BN, Bahubalendruni RM, Biswal BB, Leite M (2017) A CAD-based approach for measuring volumetric error in layered manufacturing. Proc Inst Mech Eng C J Mech Eng Sci 231(13):2398–2406. https://doi.org/10.1177/0954406216634746
27. Ferreira RTL, Amatte IC, Dutra TA, Burger D (2017) Experimental characterization and micrography of 3D printed PLA and PLA reinforced with short carbon fibers. Compos B Eng 124(Supplement C):88–100. https://doi.org/10.1016/j.compositesb.2017.05.013
28. Leite M, Varanda A, Ribeiro AR, Silva A, Vaz MF (2018) Mechanical properties and water absorption of surface modified ABS 3D printed by fused deposition modelling. Rapid Prototyping Journal 24(1):195–203. https://doi.org/10.1108/RPJ-04-2016-0057
29. Gleadall A, Ashcroft I, Segal J (2018) VOLCO: A predictive model for 3D printed microarchitecture. Addit Manuf 21:605–618. https://doi.org/10.1016/j.addma.2018.04.004
30. Fernandes J, Deus AM, Reis L, Vaz MF, Leite M (2018) Study of the influence of 3D printing parameters on the mechanical properties of PLA. In: Proceedings of the 3rd International Conference on Progress in Additive Manufacturing (Pro-AM 2018), pp. 547–552. https://doi.org/10.25341/D4988C
31. Araújo H, Leite M, Ribeiro A, Deus AM, Reis L, Vaz MF (2019) Investigating the contribution of geometry on the failure of cellular core structures obtained by additive manufacturing. Frattura ed Integrità Strutturale 13(49):478–486. https://doi.org/10.3221/IGF-ESIS.49.45
32. Miguel M, Leite M, Ribeiro AMR, Deus AM, Reis L, Vaz MF (2019) Failure of polymer coated nylon parts produced by additive

manufacturing. Eng Fail Anal 101:485–492. https://doi.org/10.1016/j.engfailanal.2019.04.005
33. Vicente C, Fernandes J, Deus A, Vaz M, Leite M, Reis L (2019) Effect of protective coatings on the water absorption and mechanical properties of 3D printed PLA. Frattura ed Integrità Strutturale 13(48):748–756. https://doi.org/10.3221/IGF-ESIS.48.68
34. Macedo RQ, Ferreira RTL, Jayachandran K (2019) Determination of mechanical properties of FFF 3D printed material by assessing void volume fraction, cooling rate and residual thermal stresses. Rapid Prototyping Journal 25(10):1661–1683. https://doi.org/10.1108/RPJ-08-2018-0192
35. Dutra TA, Ferreira RTL, Resende HB, Guimarães A (2019) Mechanical characterization and asymptotic homogenization of 3D-printed continuous carbon fiber-reinforced thermoplastic. J Braz Soc Mech Sci Eng 41(3):133. https://doi.org/10.1007/s40430-019-1630-1
36. Sardinha M, Vicente CMS, Frutuoso N, Leite M, Ribeiro R, Reis L (2020) Effect of the ironing process on ABS parts produced by FDM. Material Design & Processing Communications 151. https://doi.org/10.1002/mdp2.151
37. Dutra TA, Ferreira RTL, Resende HB, Blinzler BJ, Larsson R (2020) Expanding Puck and Schürmann inter fiber fracture criterion for fiber reinforced thermoplastic 3D-printed composite materials. Materials 13(7):1653. https://doi.org/10.3390/ma13071653
38. Saxena P, Shukla P (2021) A comprehensive review on fundamental properties and applications of poly(vinylidene fluoride) (PVDF). Advanced Composites and Hybrid Materials 4:8–26. https://doi.org/10.1007/s42114-021-00217-0
39. Slonov A, Musov I, Zhansitov A, Kurdanova Z, Shakhmurzova K, Khashirova S (2022) Investigation of the Properties of Polyphenylene Sulfone Blends. Materials (Basel) 15(18). https://doi.org/10.3390/ma15186381
40. Plisko T, Karslyan Y, Bildyukevich A (2021) Effect of Polyphenylsulfone and Polysulfone Incompatibility on the Structure and Performance of Blend Membranes for Ultrafiltration. Materials (Basel) 14(19). https://doi.org/10.3390/ma14195740
41. Dizman C, Tasdelen MA, Yagci Y (2013) Recent advances in the preparation of functionalized polysulfones. Polym Int 62(7):991–1007. https://doi.org/10.1002/pi.4525
42. Kurtz SM (2012) Chapter 6 - Chemical and Radiation Stability of PEEK. William Andrew Publishing, Norwich, pp 75–79. https://doi.org/10.1016/B978-1-4377-4463-7.10006-5
43. Li EZ, Guo WL, Wang HD, Xu BS, Liu XT (2013) Research on Tribological Behavior of PEEK and Glass Fiber Reinforced PEEK Composite. Phys Procedia 50:453–460. https://doi.org/10.1016/j.phpro.2013.11.071
44. Fabrizio M (2021) Improvement of Thermal Conditions in Extrusion Additive Manufacturing of ULTEM. Scuola di Ingegneria Industriale e Dell'Informazione. Politecnico de Milano
45. Mushtaq BMH (2019) Effect of gasoline exposure on the mechanical properties of pla and abs material processed by fused filament fabrication (fff). International Research Journal of Engineering and Technology (IRJET)
46. Veselý P, Tichý T, Šefl O, Horynová E (2018) Evaluation of dielectric properties of 3d printed objects based on printing resolution. IOP Conference Series: Materials Science and Engineering 461. https://doi.org/10.1088/1757-899X/461/1/012091
47. PLA Technical Sheet Rev3.0 (2023) 3DxTech Advanced Materials. Accessed: 14th November 2023
48. Chemical Resistance: The Ultimate 3D Printing Materials Corrosion Test, (2020). BCN3D. Accessed: 14th November 2023
49. ABS Technical Sheet Rev3.0, (2023). 3DxTech Advanced Materials. Accessed: 14th November 2023
50. PET-G Technical Sheet Rev3.0 (2023) 3DxTech Advanced Materials. Accessed: 14th November 2023
51. Technical Information bioFila Silk & Linen (2014) Lulzbot. Accessed: 14th November 2023
52. PVDF Technical Sheet Rev3.0 (2023) 3DxTech Advanced Materials. Accessed: 13th November 2023
53. Chemical Resistance PVDF (2023) Polyfluor. Accessed: 14th November 2023
54. PPSU Technical Sheet Rev3.0 (2023) 3DxTech Advanced Materials. Accessed: 14th November 2023
55. PPSF/PPSU (2023) Javelin. Accessed: 14th November 2023
56. Polyphenylsulfone (PPSU) (2023) CODI 3D Lab. Accessed: 14th November 2023
57. PEEK Technical Sheet Rev3.0 (2023) 3DxTech Advanced Materials. Accessed: 14th November 2023
58. Powering Motor Performance: An Introduction to PEEK Extrusions, (2017). Resinate. Accessed: 14th November 2023
59. Chemical Resistance PEEK (2023) Polyfluor. Accessed: 14th November 2023
60. ULTEM 1010 Technical Sheet Rev4.0, (2023). 3DxTech Advanced Materials. Accessed: 14th November 2023
61. Dielectric Strength Of Plastics Electrical Properties Of Plastics The Definitive Guide, (2023). Plastic Ranger. Accessed: 14th November 2023
62. FDM Materials - Chemical Compatibility, (2023). PStratasys. Accessed: 14th November 2023
63. PEEK-GF20 Technical Sheet Rev1.0, (2023). 3DxTech Advanced Materials. Accessed: 14th November 2023
64. Lyu Y, Zhao H, Wen X, Lin L, Schlarb AK, Shi X (2021) Optimization of 3d printing parameters for high-performance biodegradable materials. Applied Polymer Science. https://doi.org/10.1002/app.50782
65. Boytsov E, Blaginin S, Sinkov A (2022) Why we need a heated chamber for 3d printing with 'high performance' polymers? In: Modern Trends in Manufacturing Technologies and Equipment
66. Cwikla G, Grabowik C, Kalinowski K, Paprocka I, Ociepka P (2017) The Influence of Printing Parameters on Selected Mechanical Properties of FDM/FFF 3D-printed Parts. https://doi.org/10.1088/1757-899X/227/1/012033 . IOP Conference Series: Materials Science and Engineering
67. Mineral Insulating Oils Electrical Equipment - Supervision and Maintenance Guidance vol. IEC 60422:2013, (2013). International Standard. Accessed: 3rd August 2023
68. IEEE Guide for the Interpretation of Gases Generated in Mineral Oil-Immersed Transformers vol. IEEE C57.104-2019 (Revision of IEEE C57.104-1991), (2019). IEEE Standards Association. Accessed: 3rd August 2023
69. Standard Test Method for Dielectric Breakdown Voltage and Dielectric Strength of Solid Electrical Insulating Materials at Commercial Power Frequencies vol. ASTM D149-09, (2013). ASTM International. Accessed: 10th August 2023
70. Kuzmanić I, Vujović I, Petković M, Šoda J (2023) Influence of 3d printing properties on relative dielectric constant in pla and abs materials. Progress in Additive Manufacturing 6:703–710
71. Oommen TV (1984) Moisture equilibrium charts for transformer insulation drying practice. IEEE Trans Power Appar Syst PAS–103(10):3062–3067. https://doi.org/10.1109/TPAS.1984.318326